

# Ultra-Sensitive Refractive Index Sensor With Slightly Tapered Photonic Crystal Fiber

Cheng Li, Sun-Jie Qiu, Ye Chen, Fei Xu, and Yan-Qing Lu

**Abstract**—We fabricate a miniature ultra-sensitive refractive index sensor based on a tapered photonic crystal fiber (PCF) modal interferometer. The PCF is slightly tapered and a little elongated to keep the size compact. The total length is  $\sim 2$  cm, and the potential sensitivity is more than 1600 nm/RIU (refractive index unit), which is nearly eight times as high as that of an untapered PCF interferometer.

**Index Terms**—Fiber sensor, fiber taper, photonic crystal fiber (PCF), ultra-sensitivity.

## I. INTRODUCTION

REFRACTIVE index (RI) sensors have many great applications in many fields, especially in chemical industry for quality control and bio-sensing for monitoring molecular bindings. Optical fiber based RI sensors are attractive, owing to their small size, light weight, immunity to electromagnetic interference, high temperature performance, environmental ruggedness, and the ability for distributed sensing and remote sensing and in situ measurement. To date, a number of fiber RI sensors have been developed using gratings, interferometers and resonators [1]–[9]. In recent years, due to the nonconventional propagation characteristics of photonic crystal fibers (PCFs), the interferometric sensors based on PCFs built via fusion splicing and micro-hole collapsing have been demonstrated and are getting more and more attention [10], [11]. This kind of PCF based in-line modal interferometers (PCFMIs) consist of a stub of 125  $\mu\text{m}$  large-mode-area (LMA) PCF spliced between the same size standard single-mode fibers (SMFs) [10], [12]–[15]. In the spliced regions, the voids of the PCF are totally collapsed and allow the coupling and recombination of PCF core and cladding modes. Because cladding mode is sensitive to outside environment, it can be used as a RI sensor to detect the outer region of the PCF. In addition, the devices are very compact because the PCF we need is just a few centimeters and highly stable over time. The fabrication of the device is very simple, only

involving cleaving and splicing processes that can be carried out in a standard fiber optics lab. However, the sensitivity (100  $\sim$  200 nm/RIU in water) is still low due to the limited evanescent field by the large fiber size.

In this letter, we fabricate a slightly tapered PCFMI with greatly enhanced sensitivity. The air-holes of PCF aren't collapsed and the length of the device is still short and compact by little elongating the PCF. The length of PCF in our device is only  $\sim 2$  cm, and even after tapering the length is still less than 2.4 cm, so we can package such kind of device with some mechanical chucks easily. It's different from the PCF-based interferometer in [16] which makes the waist of the seriously tapered PCF totally collapsed with a low sensitivity. Moreover, the length of PCF they used is very long ( $> 30$  cm) with different interference mechanism. The RI sensing properties of our devices with different diameters of PCF are investigated experimentally. The high sensitivity of more than 1600 nm/RIU can be achieved. It is nearly eight times larger than the sensitivity of the untapered PCFMI. Of course, it is smaller than metal-based Surface Plasmon Resonance sensors, but the sensitivity is larger than other types of all-silica fiber sensors such as resonator or grating based sensors [18]. The device keeps low temperature dependence before and after tapering. More uniformly and thinly tapered PCFs can be realized with higher sensitivity by optimizing tapering process.

## II. SLIGHTLY TAPERED PCFMI

For the construction of the tapered PCFMI, we employed a commercial single mode PCF (LMA-8, NKT Photonics) consisting of a solid core surrounded by six rings of air holes. This PCF has an 8.4  $\mu\text{m}$  diameter core, voids with an average diameter of 2.17  $\mu\text{m}$  and the average separation between the voids is 5.3  $\mu\text{m}$ , these parameters are different from [16]. The diameter of the PCF is the same as SMF-28 fibers and it is cheaper and easier to be spliced to SMF-28 with higher stability and better repetition, compared with other larger size PCFs. Initially a PCF interferometer was fabricated by splicing the ends of two SMF-28 fibers to the cleaved end of a few centimeters of PCF. The voids of the PCF collapsed completely over a short region about several hundred micrometers long. Then this device was tapered by the heat-and-pull technique. Due to the same diameter, we can easily splice together the PCF and SMF-28. The length of the PCF we used is 2 cm. After the fusion splicing, the voids of the PCF around the

Manuscript received June 27, 2012; revised July 28, 2012; accepted August 15, 2012. Date of publication August 31, 2012; date of current version September 13, 2012. This work was supported in part by the National Basic Research Program of China (973 Program) under Contract 2012CB921803, Contract 2011CBA00200, and Contract 2010CB327800, in part by the National Natural Science Program of China under Contract 11074117 and Contract 60977039, in part by PADA, and in part by the National Undergraduate Innovation Program 20120284177.

The authors are with the National Laboratory of Solid State Microstructures and the College of Engineering and Applied Sciences, Nanjing University, Nanjing 210093, China (e-mail: feixu@nju.edu.cn; yqlu@nju.edu.cn).

Color versions of one or more of the figures in this letter are available online at <http://ieeexplore.ieee.org>.

Digital Object Identifier 10.1109/LPT.2012.2214379

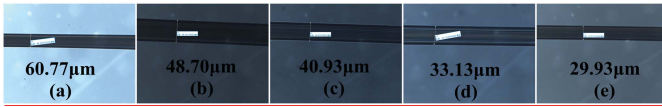


Fig. 1. Images of the waists of the slightly tapered PCFs. (a)–(e) Magnifications are 4, 10, 10, 25, 25 times and the waist diameters are 61, 49, 41, 33, and 30  $\mu\text{m}$ , respectively.

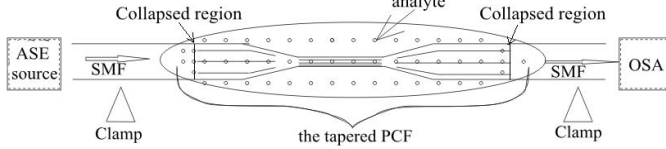


Fig. 2. Schematic of the experimental setup for interference spectra and RI sensing measurement.

ends were totally collapsed over a short region about several hundred micrometers long. Then we slightly stretched the PCF which was heated by a hydrogen flame torch. We can control the velocity and the displacement of the electric translation stages to make different diameters of the PCFs. We tapered the samples with different diameters as shown in Fig. 1. The waist diameters are 61  $\mu\text{m}$  (Fig. 1(a)), 49  $\mu\text{m}$  (Fig. 1(b)), 41  $\mu\text{m}$  (Fig. 1(c)), 33  $\mu\text{m}$  (Fig. 1(d)), and 30  $\mu\text{m}$  (Fig. 1(e)), respectively. The waists of these tapered PCFs are not collapsed and only a little elongated. Even when the waist diameter is tapered to 30  $\mu\text{m}$ , the length of the PCF is only 0.4 cm longer than the untapered one.

### III. INTERFERENCE SPECTRA

Optical characterization of the tapered PCFMI is performed using an Ando AQ6317B optical spectrum analyzer (OSA) accompanied by an amplified spontaneous emission (ASE) source (1525 ~ 1610 nm) as shown in Fig. 2. When light travels from the SMF to the tapered PCF in the interferometer, the SMF fundamental mode begins to diffract. When it enters the collapsed PCF region, it excites core and cladding modes in the PCF section with different propagation constants [10]–[13]. After propagating in the PCF, the modes reach the other collapsed end of the PCF. They will thus further diffract and will be recombined through the filtering of the subsequent SMF. Therefore, the transmission of our interferometer can be expressed as that of a two-mode interferometer [17]

$$I = I_{co} + I_{cl} + 2\sqrt{I_{co}I_{cl}} \cos(\delta + \varphi_0) \quad (1)$$

$$\text{Free spectral range (FSR)} = 2\pi\lambda/\delta \quad (2)$$

where  $\delta = (2\pi/\lambda) \int_L^{(n_{cl}-n_{co})} dz$ ,  $I$  is the intensity of the interference signal,  $I_{co}$  and  $I_{cl}$  are the intensities of the core and cladding modes.  $\delta$  is the phase difference of the two modes;  $n_{co}$  and  $n_{cl}$  are the effective indices of the core and cladding modes, which depend on the diameter  $D$  of the tapered PCF.  $L$  and  $\lambda$  are the PCF length and the wavelength, respectively.

Figure 3 shows the measured interference spectra of a PCFMI before and after tapering in air. The waist diameters are 125  $\mu\text{m}$ , 61  $\mu\text{m}$  and 33  $\mu\text{m}$ , respectively. It looks like the spectra of multiple-mode interference possibly because

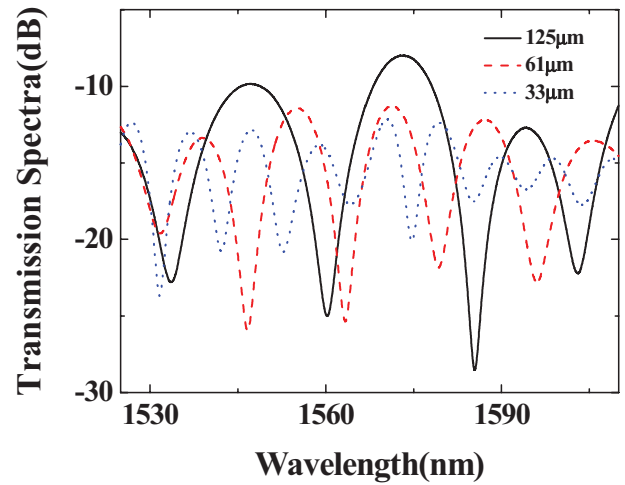


Fig. 3. Spectra of the untapered (solid line) and tapered (dashed and dotted) PCFMIs.

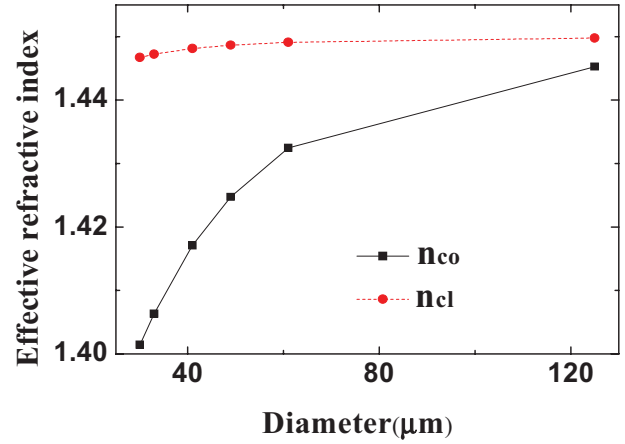


Fig. 4. Effective refractive index of the core and first cladding modes at different diameters.

more than one cladding modes are excited. For simplicity, we use two predominant modes interference around 1550 nm to describe the interference. The FSR decreases when the diameter decreases because  $n_{cl}$  is little changed while  $n_{co}$  decreases rapidly, as shown in Fig. 4. In our experiment, the FSR around 1550 nm we get are 27 nm (125  $\mu\text{m}$ ), 17 nm (61  $\mu\text{m}$ ), 11 nm (33  $\mu\text{m}$ ), respectively. They agree with the theoretical results which are 26 nm (125  $\mu\text{m}$ ), 19 nm (61  $\mu\text{m}$ ), 10 nm (33  $\mu\text{m}$ ) from Eq. (2). The minor difference is because we calculate the FSR using measured  $L$  with micrometer accuracy and assuming the tapered PCF is uniform with the same waist diameter. In fact, the tapered PCF is un-uniform because of the taper transition. Then the calculated results are slightly different with the measured results.

Due to the taper transition region is nonadiabatic, the loss of the cladding mode will increase with diameter decreasing. According to the formula (1), the contrast ratio will be bad. From Fig. 3, we can see that the contrast ratio decreases with decreasing diameter. But even when the diameter of the taper is 33  $\mu\text{m}$ , the contrast ratio is more than 10 dB.

The performance of interferometer RI sensors can be evaluated by using the sensitivity  $S$ , which is defined as the

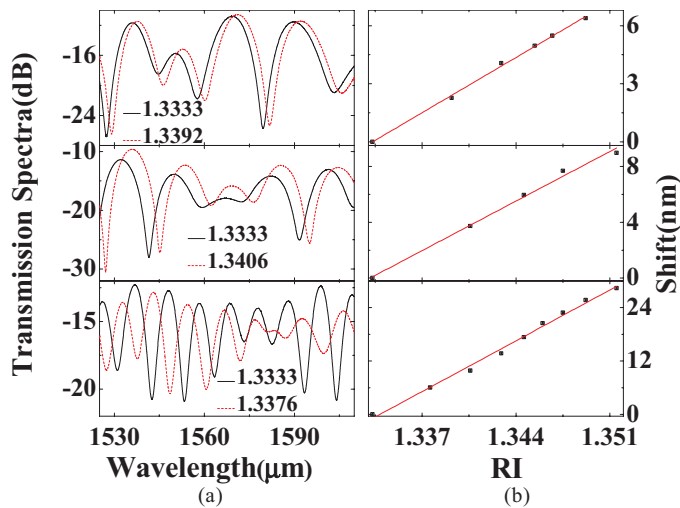


Fig. 5. (a) Transmission spectra and (b) wavelength shift as a function of the surrounding RI of three tapered PCFs with  $D = 61 \mu\text{m}$  (top plots),  $49 \mu\text{m}$  (middle plots), and  $30 \mu\text{m}$  (bottom plots).

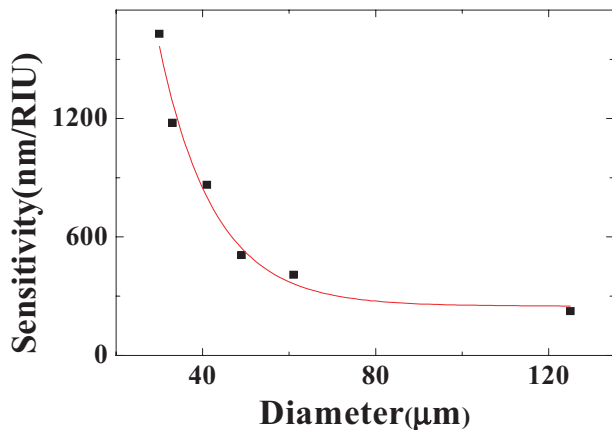


Fig. 6. Sensitivity of PCFs with different diameters.

magnitude in shift of the resonant wavelength divided by the change in refractive index of the analyte. The sensitivity was measured by inserting these PCFMI in water and mixtures of water and acetone. These solutions were chosen with the objective of simulating aqueous solutions, having a refractive index in the region around 1.33 at the wavelength of  $1.55 \mu\text{m}$ . We mainly detect the index range around 1.34. We choose the water component with the following ratios: 1, 10/12, 10/14, 10/16, 10/18, 10/20, 8/18, 6/16 and 4/14. The RIs of water and acetone at  $1.55 \mu\text{m}$  are 1.3333 and 1.3577, respectively [17].

In the left-hand graph of Fig. 5, we show the interference pattern in water with three different waist diameters,  $61 \mu\text{m}$  (top),  $49 \mu\text{m}$  (middle) and  $30 \mu\text{m}$  (bottom). As RI increases, the spectrum shows a red-shift. The right-hand graph of Fig. 5 shows the wavelength shift as a function of the surrounding RI. The asterisks represent the measurement results while the solid line is the best-fitting. The sensitivities are  $408 \text{ nm/RIU}$ ,  $507 \text{ nm/RIU}$ , and  $1629 \text{ nm/RIU}$ , respectively. The sensitivity increases much after tapering.

Figure 6 shows the sensitivity of the PCFs with different diameters. Therefore we can get the information that with

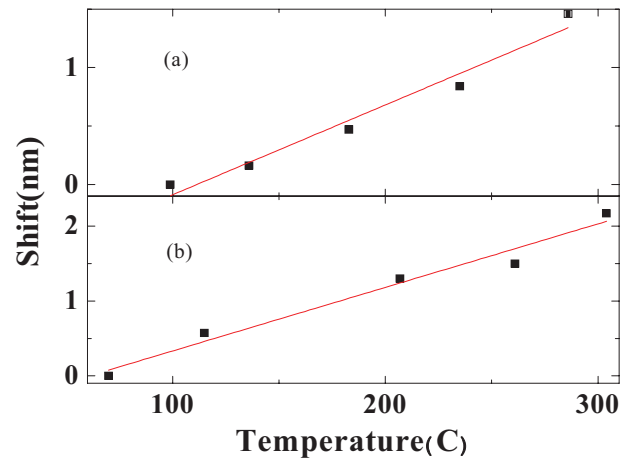


Fig. 7. (a) Wavelength shift of the untapered PCF and (b)  $33\text{-}\mu\text{m}$ -diameter tapered PCF due to the temperature change.

the decrease of the diameter of PCF, the sensitivity increases rapidly. And the sensitivity can exceed  $1600 \text{ nm/RIU}$  with  $30 \mu\text{m}$ -diameter taper. It is nearly eight times larger than the sensitivity of the untapered PCFMI which is  $223 \text{ nm/RIU}$ .

Furthermore, we also observed the spectra of the untapered PCF and  $33 \mu\text{m}$ -diameter tapered PCF in different temperatures. Figure 7(A) is the wavelength shift of the untapered PCF due to the temperature change and the fitted value is  $7.68 \text{ pm/}^\circ\text{C}$ . Figure 7(B) is the wavelength shift of the  $33 \mu\text{m}$ -diameter tapered PCF due to the temperature change and the fitted value is  $8.49 \text{ pm/}^\circ\text{C}$ . Take the error of the thermometer into consideration, the temperature sensitivity changed little after stretched.

#### IV. CONCLUSION

We fabricate a miniature ultra-sensitive RI sensor based on a tapered PCFMI. The PCF is slightly tapered and the length is a little elongated (less than  $2.4 \text{ cm}$ ). RI sensitivity can be achieved more than  $1600 \text{ nm/RIU}$  after tapering, much higher than recent results utilizing the same mechanism [10]–[12]. Furthermore, we also find the temperature sensitivity changed little after stretched. Ref. [16] reported another kind of tapered-PCF-based interferometer with different schematic and working mechanism. Its length is more than  $30 \text{ cm}$ . It does not need splice the PCF to SMF and it can only work depending on the PCF itself. The losses introduced by the tapering of their PCFs are less than  $3 \text{ dB}$ . But the sensitivity is less than  $1200 \text{ nm/RIU}$  in water at the diameter of  $\sim 30 \mu\text{m}$ . Compared with it, the device we made is much more compact and less cost with higher sensitivity. More uniform and thinner tapered PCFMI can be realized with higher sensitivity by optimizing the tapering process.

#### REFERENCES

- [1] P. Wang, G. Brambilla, M. Ding, Y. Semenova, Q. Wu, and G. Farrell, "High-sensitivity, evanescent field refractometric sensor based on a tapered, multimode fiber interference," *Opt. Lett.*, vol. 36, no. 12, pp. 2233–2235, 2011.
- [2] K. Mileňko, *et al.*, "Photonic crystal fiber tip interferometer for refractive index sensing," *Opt. Lett.*, vol. 37, no. 8, pp. 1373–1375, 2012.

- [3] D. J. J. Hu, L. J. Long, W. Yixin, and P. P. Shum, "Miniaturized photonic crystal fiber tip sensor for refractive index sensing," in *Proc. IEEE Sensors*, Oct. 2011, pp. 1488–1490.
- [4] F. Xu and G. Brambilla, "Demonstration of a refractometric sensor based on optical microfiber coil resonator," *Appl. Phys. Lett.*, vol. 92, no. 10, pp. 101126-1–101126-3, 2008.
- [5] A. N. Chryssis, S. M. Lee, S. B. Lee, S. S. Saini, and M. Dagenais, "High sensitivity evanescent field fiber Bragg grating sensor," *IEEE Photon. Technol. Lett.*, vol. 17, no. 6, pp. 1253–1255, Jun. 2005.
- [6] F. Xu, G. Brambilla, and Y. Lu, "A microfluidic refractometric sensor based on gratings in optical fibre microwires," *Opt. Express*, vol. 17, no. 23, pp. 20866–20871, 2009.
- [7] I. M. White, H. Oveys, and X. Fan, "Liquid-core optical ring-resonator sensors," *Opt. Lett.*, vol. 31, no. 9, pp. 1319–1321, 2006.
- [8] H. Xuan, W. Jin, and M. Zhang, "CO<sub>2</sub> laser induced long period gratings in optical microfibers," *Opt. Express*, vol. 17, no. 24, pp. 21882–21890, 2009.
- [9] A. C. Boucouvalas and G. Georgiou, "External refractive-index response of tapered coaxial couplers," *Opt. Lett.*, vol. 11, no. 4, pp. 257–259, 1986.
- [10] R. Jha, J. Villatoro, G. Badenes, and V. Pruneri, "Refractometry based on a photonic crystal fiber interferometer," *Opt. Lett.*, vol. 34, no. 5, pp. 617–619, 2009.
- [11] R. Jha, J. Villatoro, and G. Badenes, "Ultrastable in reflection photonic crystal fiber modal interferometer for accurate refractive index sensing," *Appl. Phys. Lett.*, vol. 93, no. 19, pp. 191106-1–191106-3, 2008.
- [12] S.-J. Qiu, Y. Chen, J.-L. Kou, F. Xu, and Y.-Q. Lu, "Miniature tapered photonic crystal fiber interferometer with enhanced sensitivity by acid microdroplets etching," *Appl. Opt.*, vol. 50, no. 22, pp. 4328–4332, 2011.
- [13] J. Villatoro, V. Finazzi, G. Badenes, and V. Pruneri, "Highly sensitive sensors based on photonic crystal fiber modal interferometers," *J. Sensors*, vol. 2009, pp. 747803-1–747803-11, Jun. 2009.
- [14] S.-J. Qiu, Y. Chen, F. Xu, and Y.-Q. Lu, "Temperature sensor based on an isopropanol-sealed photonic crystal fiber in-line interferometer with enhanced refractive index sensitivity," *Opt. Lett.*, vol. 37, no. 5, pp. 863–865, 2012.
- [15] J. Villatoro, V. P. Minkovich, V. Pruneri, and G. Badenes, "Simple all-microstructured-optical-fiber interferometer built via fusion splicing," *Opt. Express*, vol. 15, no. 4, pp. 1491–1496, 2007.
- [16] V. Minkovich, *et al.*, "Holey fiber tapers with resonance transmission for high-resolution refractive index sensing," *Opt. Express*, vol. 13, no. 19, pp. 7609–7614, 2005.
- [17] J.-L. Kou, J. Feng, Q.-J. Wang, F. Xu, and Y.-Q. Lu, "Microfiber-probe-based ultrasmall interferometric sensor," *Opt. Lett.*, vol. 35, no. 13, pp. 2308–2310, 2010.
- [18] O. Esteban, N. Díaz-Herrera, M.-C. Navarrete, and A. González-Cano, "Surface plasmon resonance sensors based on uniform-waist tapered fibers in a reflective configuration," *Appl. Opt.*, vol. 45, no. 28, pp. 7294–7298, 2006.